

High-capacity stacking apparatus for thermoforming machine – Part II: Structural design of the adjustable stacker driving mechanism

Marko Penčić¹, Maja Čavić¹, Dragana Oros, Dijana Čavić,
Marko Orošnjak and Velibor Karanović

Abstract

Part II presents the structural design of a high-capacity adjustable stacker mechanism for thermoforming machines which enables the receipt, transport and stacking of cup-like products. It was previously established (please see Part I) that a four-bar linkage mechanism with a one-way clutch is the optimal solution for realizing the intermittent motion of the stacker conveyor. The main objective here is to enable the change of the stacker work parameters, with the goal of changing and adjusting the work stroke of the conveyor. Accordingly, there are two main requirements the solution needs to fulfill. The first is that of the regulation characteristic's function – the relationship between the change of the work stroke and the change of the regulation parameter, must be linear, and the second is that it allows for regulation within a wide range. Due to this, the adopted solution proposed that two links have variable lengths. The input link should have discrete length values which correspond to different values of the conveyor work stroke, while the output link length should be continuously variable, within a narrow range thus ensuring linear regulation characteristic. Finally, it should be noted that this solution makes the stacker compatible with a wide array of products, which increases the productivity and flexibility, adjusting the stacker to receive a different product can be done quickly and easily and avoiding a halt in the production as it takes less time to adjust the stacker than the thermoforming machine.

Keywords

Thermoforming machine, high-capacity stacking apparatus, structural design, adjustable four-bar linkage mechanism, one-way clutch, intermittent motion, adjustable work stroke, work coefficient

Date received: 8 April 2021; accepted: 22 September 2021

Handling Editor: Chenhui Liang

Introduction

Contemporary high-capacity thermoforming machines are unable to work efficiently without a stacker to receive and stack the formed products, such as single-use petroplastic packaging. The stacker can be integrated into the thermoforming machine as the final station, or a completely independent machine positioned at the output of the thermoforming machine. Regardless of the level of automation, a key stacker parameter is the productivity, defined as the number of

products the stacker can receive and stack in the prescribed time. The capacity of the stacker largely depends on the size of the mould and the capacity of the thermoforming machine, with the stacker's capacity

Faculty of Technical Sciences, University of Novi Sad, Novi Sad, Serbia

Corresponding author:

Maja Čavić, Faculty of Technical Sciences, University of Novi Sad, Trg
Dositaja Obradovića 6, Novi Sad 21000, Serbia.
Email: scomaja@uns.ac.rs



Creative Commons CC BY: This article is distributed under the terms of the Creative Commons Attribution 4.0 License (<https://creativecommons.org/licenses/by/4.0/>) which permits any use, reproduction and distribution of the work without further permission provided the original work is attributed as specified on the SAGE and Open Access pages (<https://us.sagepub.com/en-us/nam/open-access-at-sage>).

needing to be equal or higher than that of the thermoforming machine. Otherwise, products accumulate, which can lead to a stop in the production. A solution to this problem could be found in increasing the stacker's buffer size or its operating speed, which decreases the life expectancy of the stacker's parts. Another important parameter is the stacker's flexibility – the possibility of using the same stacker for a wide range of different products with minimal adjustments to the working parts of the stacker. Changing the size and shape of the product necessitates changing the mould, which changes the working parameters of the thermoforming machine. Since the stackers need to work in sync with the machine, the stackers working parameters need to be changed as well. Furthermore, adjusting the stacker should be simple and fast, specifically faster than the time required to change the mould of the thermoforming machine. Another point to consider is the fact that customers that already own a thermoforming machine usually choose to buy their stacker from the same manufacturer. If this is not the case, the stacker's price becomes the deciding factor, regardless of the stacker's other characteristics, such as the work cycle, buffer size, etc.

According to the previously elaborated points, the main characteristics of a thermoforming machine stacker are: (i) high productivity, (ii) the possibility of implementation with thermoforming machines from an array of different manufacturers, (iii) simple kinematic structure and modular design, (iv) high stacking rate, (v) adjustable work stroke, (vi) high buffer capacity, (vii) compatibility with a wide variety of products with minimal adjustment of working elements, (viii) low manufacturing cost and (ix) low energy consumption. All this makes the design and realization of a thermoforming machine stacker a serious challenge.

Part I presented the type and dimension synthesis of different simple structure mechanisms that could generate the motion of the stackers working elements, with the four-bar linkage in combination with a one-way clutch (OWC) mechanism being the optimal solution to drive the stacker.¹ Part II shows the structural design of the adjustable driving mechanism for a mechanical stacker used for the receipt, transport and stacking of cylindrical, axially symmetrical petroplastic packaging. The main objective of this paper is to provide the adjustment of working parameter of the stacker – the conveyor work stroke, during constant input. The ability to adjust the mechanisms working parameters represents a significant aspect of the stacker's flexibility, as it makes the stacker compatible with a wide range of different products, increasing its productivity and efficiency.

The paper is structured as follows. The first section explains the motivation and end goal of the research. The second section reviews existing patents of stackers

from reputable manufacturers of thermoforming machines and state of the art in the field of the adjustable mechanisms. The third section defines the issues that arise with the adjustment of the stacker which ensure its compatibility with different products. The fourth section shows the structural design of the stacker, as well as the different ways of changing and adjusting the work stroke of the conveyor. A summary and discussion of the results are shown in section five, while the final section contains the conclusions and possible directions for future research.

State of the art

Part II considers the possibility of making the adopted four-bar mechanism adjustable, allowing the change and adjustment of the conveyor work stroke, during constant input speed of the motor. The core issue in Part II is finding a way to adjust one or more of the mechanism links to achieve a wider interval of possible work strokes, as well as making the change linear along the whole possible work stroke interval, which requires compromising on a number of parameters. Accordingly, a review of existing literature was done and includes three problem groups: (i) a review of existing stacker patents, where it should be noted that it was ascertained that there are no papers showing the design and kinematics of stackers, which steered the review heavily towards patents from reputable manufacturers of thermoforming machines, (ii) practical uses of adjustable mechanisms and (iii) optimum synthesis of adjustable four-bar mechanisms.

A lever-based stacker for accepting, rotating, and stacking formed cup-like products into vertical columns is shown in Hittig and Wölk²; when the columns are filled, the stacker mechanism rotates and occupies a horizontal position by moving the grouped products to the receiving plate or conveyor for packaging. A stacking station for thermoformed cup-like products is shown in Wieser and Knoll³; thermoformed products are ejected onto the stacker conveyor belt, which transports them to the product manipulation device; the products are further grouped, stacked into each other, after which they are positioned for packaging. A machine for stacking thermoformed products is shown in Trautwein et al.⁴; it consists of a magazine for accepting formed products and a system for manipulating the magazines; the products are brought into the storage position by rotating the ejector; after that, the filled magazines are moved and positioned for emptying and packaging of the stacked products. The stacking of thermoformed lids by way of gravity without the use of buffers is shown in Lederer⁵; namely, the lids are grouped into piles so that each subsequent lid fits into the previous one and pushes it to the limiter; after the

formed piles reach the defined height, they are removed from the magazine and forwarded for packaging. A device for stacking thermoformed products in vertical piles is shown in Wölk and Zabel⁶; it consists of buffers and devices for manipulating grouped products; the buffer contains two plates for receiving and stacking products; after the vertical pile reaches the defined height, the products are moved to the manipulation device; this device allows the rotation of grouped products in a horizontal position, for packaging. A thermoforming machine with an integrated stacking station is shown in Benker and Llewellyn⁷; the stacker, a magazine with several positions for storing products, is located above the ejector; thus, the ejector pushes the products up directly into the stacker; when the stacker magazine is full, emptying is done manually or by changing the magazine, which implies a delay in production. A device for handling and stacking previously grouped A-B-C products is shown in Padovani⁸; A-B-C products include thermoformed containers or lids with at least three protrusions or spacers for stacking; pre-grouped A-B-C products are stacked by ejection up into the stacker space to a predefined height. A thermoforming machine with an integrated stacker (but not as a machine station) is shown in Padovani⁹; after thermoforming, the products are transported from the ejector to the receiving mould-like plates; in addition, the receiving plates move in cycles in accordance with the thermoforming machine cycle.

The configuration synthesis of a guide-bar mechanism coupled with the link whose length can be adjusted to design a variable stiffness mechanism is shown in Shao et al.¹⁰; the movement of the guide bar mechanism is limited by the linear spring, while the length-adjustable link is used to adjust the stiffness. The design of an adjustable slider-crank mechanism to simultaneously generate a function and path on an output link, with variable input and offset link lengths, but without a limit on the number of precision points, is shown in Dutta and Naskar.¹¹ A kinematic analysis of a reconfigurable four-legged mechanism with 1 DOF to ensure the stability of the mechanism with minimal power consumption of the drive is shown in Krishnaraju and Abdul Zubar.¹² The development of an assistive adjustable rolling cam mechanism for a knee joint in the elderly is shown in Choi et al.¹³; the knee mechanism is implemented by connecting several rolling cams with precisely calculated contact geometry. The synthesis and analysis of a steering system of an adjustable tread-width four-wheel tractor are shown in Simionescu and Talpasanu.¹⁴ The synthesis and experimental validation of an adjustable six-bar crank-rocker-slider mechanism in piston-axial pumps with a variable plate angle are shown in Wilhelm and Van de Ven.¹⁵ The development of an adjustable knee joint based on a four-bar linkage mechanism for the rehabilitation of patients with the problem of lower leg activation is shown in Olinski

et al.¹⁶; the authors added two identical two-bar modules to generate a complex movement of the lower leg, i.e. for rotation of the lower leg about the horizontal and vertical axis. Adjustable four-bar articulated-leg-wheel subsystem with on-line change of subsystem parameters to overcome obstacles and control on uneven terrain is shown in Alamdari et al.¹⁷ A new type of passive power-source-free stiffness-self-adjustable mechanism representing the elbow joint of a robotic arm is shown in Liu et al.¹⁸; it should be noted that the stiffness of the mechanism is self-adjusting by pure mechanics, while the experimental confirmation of the analytical stiffness model was tested on a prototype. An arm muscle rehabilitation mechanism based on a statically balanced spring mechanism, without a driving motor, with adjustable load capability is shown in Lucieer and Herder¹⁹; a very important part of the mechanism is a wrapping cam with variable transmission which is minimized by rolling friction on the support plane. The design of an adjustable exoskeleton foot mechanism consisting of a slider-crank and a cam mechanism for generating an accurate and easily adjustable walking path is shown in Thongsookmark et al.²⁰

A design method based on changing the speed trajectory and input link length to improve or obtain the output motion characteristics of a four-bar mechanism with 1 DOF is shown in Soong²¹; the flexibility of the application of the mechanism is realized by adjusting the length of the driving link. The synthesis of a planar five-bar slider mechanism with variable topology using dyad techniques is shown in Daivagna and Balli²²; the synthesis is done for three positions in Phase I (the crank is fixed temporarily) and for two positions in Phase II (the slider is fixed temporarily). Dimensional synthesis of an adjustable four-bar mechanism to generate an accurate and continuous square path is shown in Govindasamy et al.²³; the optimization was done using the method of genetic algorithm as well as pattern search algorithm. The kinematic synthesis of a four-bar mechanism with an adjustable moving pivot for multi-phase motion generation is shown in Wang and Sodhi²⁴; the mechanism can fulfill a maximum of five prescribed positions of movement, so a numerical method for solving a given problem has been developed. Generating filleted rectangular paths using an adjustable four-bar linkage mechanism is shown in Ganesan and Sekar²⁵; the key points of the generated path were confirmed using the reconstructed adjustable parameter curve method, while the synthesis of dimensional parameters of the adjustable mechanism was done using the genetic algorithm and pattern search method. The synthesis of a four-bar mechanism with adjustable crank length when the coupler point (end-effector) moves along a set of desired paths in the plane is shown in Ibrayev et al.²⁶; the applied method is based on the least square approximation, allowing the design

of the mechanism without restrictions in the number of desired paths and the number of prescribed positions on each path; in combination with the random search technique, this method allows finding all local minima of the optimized objection function and thus can take full advantage of the considered mechanism structure. The synthesis of an adjustable four-bar linkages for precise generation of continuous paths by setting 1 DOF parameter using a genetic algorithm is shown in Zhou and Castillo.²⁷ A new methodology for the synthesis of adjustable planar four-bar crank-rocker mechanisms for approximate multi-path generation is presented in Chanekar and Ghosal²⁸; in order to obtain optimal design variables, the sequential quadratic optimization algorithm was used where the objective function includes the smallest possible number of variables. The optimal synthesis method of adjustable four-bar linkages for generating multi-phase motion is shown in Zhou and Cheung²⁹; requirements related to fixed pivot positions, no branch defect, crank existence and link length ratio are taken as restrictions; after the synthesis of adjustable four-bar linkages, the transmission angle should be optimal for which the modified genetic algorithm method was used. Two synthesis methods of a four-bar mechanism with two pairs of trajectory curvature and velocity have been proposed in Chang³⁰; using the concept of cross-ratio, constraint equations and useful properties of the mechanism are formed; in addition, special cases are considered when the mechanism is a crank-rocker or slider-crank type. Optimal dimensional synthesis of a rhombus path generating adjustable four-bar mechanism using the reconstructed adjustable parameter curve method is shown in Govindasamy et al.³¹; the optimal solution for the precise generation of a rhombus-shaped path was obtained using a genetic algorithm and a pattern search method. Optimal synthesis of adjustable four-bar mechanism for precisely generated desired continuous paths with optimal length adjustment 1 DOF link is shown in Zhou et al.³²; length adjustment is performed on a driven side link or coupler within a four-bar mechanism, while the optimal solution is obtained using a genetic algorithm.

Based on the review of existing patents, none of the described solutions considers the possibility of mechanically adjusting the stackers working parameters, which potentially lowers the number of products the stacker can interact with. In adjustable mechanisms, some of their constructive parameters are changed in order for the mechanism to perform the desired property or task. Such mechanism can be found in different areas such as robotics, medical engineering, automotive engineering, etc., and are the subject of intensive research. Simple structure linkages are the ones most often used. This is due to the fact that the design parameters being adjusted are link lengths and fixed joint positions, which is very easy to realize in practise. Changing the

cam of a cam mechanism is economically irrational, so adjustable cam mechanisms are usually used in combination with tendons where cams function as pulleys. Cam mechanisms can be made adjustable by changing other design parameters – the position of the fixed joints, the length of the follower lever, etc. The problem most often considered is the generation of differently shaped trajectories, as well as families of similar ones, usually by changing only one design parameter, most often the position of a fixed joint, which makes the most sense from a practical point of view. Changing the length of links is done by combining the link with a grooved cam. The practical realisation of adjustable design parameters is rarely considered, despite its significance. Since the problem in question is quite complex and requires the consideration of a number of interconnected influences, the solving is usually done using optimization methods and their combinations.

Due to all of the statements above, we propose a high-capacity mechanical stacker with the possibility of adjusting working parameters – the work stroke, specifically. The driving mechanism of the stacker consists of an adjustable four-bar linkage. Adjustment of the stacker work stroke will be realized by changing the design parameters of the driving mechanism. All possible options for regulation parameters will be explored and the optimum one will be adopted. Also, viability of the practical realization will be regarded as key factor in the design.

Problem description

Figure 1 shows the working principle of a stacker meant to receive, transport and stack thermoformed cup-like products. The products are ejected from the mould (11) of the thermoforming machine using pressurized air and gravitationally drop down onto interconnected panels (9) which form the conveyer of the stacker. Every panel contains holes with a diameter smaller than the top diameter of the product. Due to this, the products fall into the holes on the panels due to their own weight and shape. It should be noted that the height of individual products is not limited, which is a great advantage over a large number of commercial solutions. Also, with sufficient number of panels, stacker can receive all products from the machine thus allowing to be to function independent of the machine cycle. Moving on, the designation W represents panel width which must be slightly larger than the hole diameter, while distance S between the hole centres on adjacent panels represents the work stroke of the stacker. Distance S is the sum of the value W and the distance between two panels; for example for top diameter of 50 mm, hole diameter is 46 mm, so $W = 46 + 2\delta = 52$ mm and $S = W + \lambda = 56$ mm, where $\delta = 3$ mm – distance

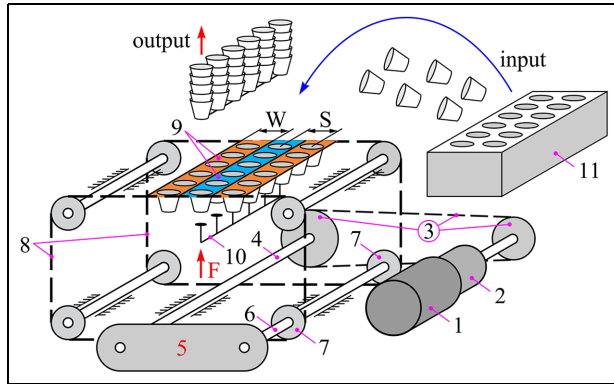


Figure 1. Schematic representation of a stacker for cup-like products: 1 – actuator, 2 – gearbox, 3 – chain drive, 4 – input/driving shaft, 5 – stacker mechanism that provides intermittent motion, 6 – output/driven shaft, 7 – conveyor driving sprockets, 8 – chains, 9 – panels, 10 – puncher and 11 – mould.

between the panel and the hole, and $\lambda = 4$ mm – distance between two adjacent panels. With each stroke, the conveyor positions the products above a pneumatic puncher (10) that pushes the products upwards, forming a number of stacks. It should be noted that it is not an issue if a hole does not have a product in it when it gets to the puncher, since each vertical stack has no individual limit in the number of products it can contain before it is removed for packaging. If a product does not fall into any of the holes, it is stopped from moving further down the conveyor with a barrier, like a curtain for example. The product is then returned to the beginning of the conveyor using pressurized air. During the ejection of the products from the holes, the conveyor should be standing still. Therefore, the conveyor's motion must be intermittent, with periods of motion and dwell that correspond to the work cycle of the thermoforming machine. This makes the intermittent motion of the conveyor basic requirement in the design of the stacker.

The stacker's drive consists of the constant rpm actuator (1), gearbox (2), chain transmission (3) and driving shaft (4). This shaft is the input of the mechanism (5) which transforms the continuous rotation of the input link into the intermittent motion of the output link – the driven shaft (6). Fixed to the driven shaft (6) are the sprockets (7) which, with the use of chains (8), move the panels (9). The main objective – the transformation of the continuous motion of the input into the intermittent motion of the output, is fulfilled by the mechanism (5).

Another equally important design requirement is the flexibility of the stacker. Namely, there is no universal standard for the dimensions and shape of single-use plastic products. It is fully dependent on the design of the manufacturer and customer demand, which brings innovative influences to the design, as the manufacturers try their best to keep their products distinguishable among a plethora of similar products. As an additional

Table 1. Typical size of single-use axially symmetrical petroplastic packaging products.

Application	Size [oz]	Volume [mL]	Diameter		Height [mm]
			Top* [mm]	Base [mm]	
Plastic cold cups	4	120	66 (59)	45	60
	6.5	200	66 (59)	45	95
	8	240	66 (59)	50	105
			98 (91)	50	65
	10	300	82 (75)	50	100
			98 (91)	55	75
	12	360	82 (75)	55	110
			98 (91)	55	85
Plastic portion cups	16	480	82 (75)	60	135
			98 (91)	65	100
	0.5	15	50 (43)	35	15
	0.75	22	50 (43)	30	22
	1	30	50 (43)	30	30
	1.5	45	66 (59)	45	22
	2	60	66 (59)	45	30
	2.5	75	66 (59)	40	40
	3	90	66 (59)	40	47
	3.25	100	82 (75)	55	32
	4	120	82 (75)	50	40
	5.5	165	82 (75)	50	55

The values outside the parentheses account for the rim of the cup.

option, the packaging manufacturer allows the customer to further customize the design, but only in accordance with the capabilities of the thermoforming machine and the selected packaging materials. Due to this, cups that have the same volume can significantly differ in shape and dimensions. Table 1 shows the typical size of a number of single-use axially symmetrical petroplastic packaging products.

Although there is an infinite number of possible shapes and dimensions of plastic cups, some limitations do exist and are defined by the stretching and shaping characteristics of thermoplastic foil. These foil characteristics are defined by the appropriate standards, such as the hazard analysis critical control point (HACCP). As long as the predefined characteristics (foil thickness, stretching of the foil, etc.³³) are satisfied, the customer is free to define the aesthetic characteristics of the packaging, such as the addition of a smooth rim, the volume, height and top and bottom diameters.³⁴ To conclude, in order to make the stacker compatible with products of different shapes and sizes, the work stroke of stacker has to be adjusted. The regulation has to be realized by changing the design parameters of the stacker driving mechanism in way that makes it practically achievable. The following section shows the structural design of a stacker mechanism that transforms the continuous input motion into intermittent output motion, as well as the regulation of the intermittent output motion.

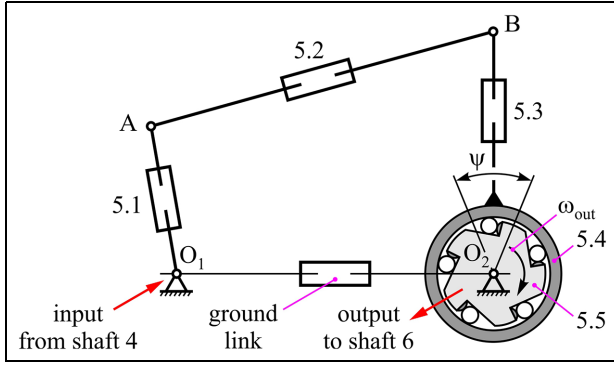


Figure 2. Schematic representation of stacker mechanism.

Stacker driving mechanism

Figure 2 shows the motion transformation mechanism which consists of a four-bar linkage and a OWC mechanism. The four-bar linkage consists of the driving link – input link (5.1), the connecting link (5.2) and the output link (5.3), which is fixed to the outer ring (5.4) – the input link of the OWC, while the star or inner ring (5.5) – the output link of the OWC, transmits power and motion to the driving sprocket of the conveyor. The input link of the four-bar linkage continuously rotates, while the output link oscillates. The existence of transmission of power and motion to the inner ring of the OWC, as well as to the driving sprockets, depends on the output link oscillation direction.

The stroke S of the stacker directly depends on the motion interval of the output link – angle ψ , while this angle depends on the lengths of the four-bar linkage links. To change the stroke, one link will be chosen and its length changed to achieve different motion interval values, changing the stroke of the stacker. A limitation to the stroke value is that it has to be bigger than the top diameter of the product. According to Table 1, the minimum and maximum stroke (distance S , see Figure 1) values are adopted as 56 and 104 mm, respectively. The median stroke value corresponds to the median motion interval value, so:

$$\psi_{sr} \leftrightarrow \frac{104 + 56}{2} = 80 \text{ mm} = S_{sr} \quad (1)$$

The minimum and maximum stroke values correspond to the minimum and maximum motion interval values, so:

$$\psi_{min} = \psi_{sr} - \Delta\psi \leftrightarrow 56 \text{ mm} = S_{min} \quad (2)$$

$$\psi_{max} = \psi_{sr} + \Delta\psi \leftrightarrow 104 \text{ mm} = S_{max} \quad (3)$$

where:

$$\Delta\psi = \pm \left(\frac{104 - 56}{2} \right) \frac{\psi_{sr}}{80} = \pm 0.30\psi_{sr} \quad (4)$$

According to equation (4), the range of regulation is $\pm 30\%$ of the median value of the motion interval ψ_{sr} , making the total motion interval:

$$\psi = \psi_{sr} \pm \Delta\psi \quad (5)$$

For the previously explored motion intervals of the output link, the following relations are adopted:

- for $\psi_{sr} = 15^\circ$, $\Delta\psi$ is $\pm 5^\circ$, so the adjustable range is of angle ψ is $10^\circ \div 20^\circ$,
- for $\psi_{sr} = 30^\circ$, $\Delta\psi$ is $\pm 10^\circ$, so the adjustable range is of angle ψ is $20^\circ \div 40^\circ$,
- for $\psi_{sr} = 45^\circ$, $\Delta\psi$ is $\pm 15^\circ$, so the adjustable range is of angle ψ is $30^\circ \div 45^\circ$,
- for $\psi_{sr} = 60^\circ$, $\Delta\psi$ is $\pm 20^\circ$, so the adjustable range is of angle ψ is $40^\circ \div 80^\circ$.

Changing the motion interval directly impacts the stacker stroke, meaning that:

$$S = iR\psi = iR(\psi_{sr} \pm \Delta\psi) = iR\psi_{sr} \pm iR\Delta\psi = S_{sr} \pm \Delta S \quad (6)$$

where: i is the transmission ratio between the inner ring of the OWC and the driving sprocket of the conveyor, while R is the radius of the driving sprocket.

If the relation between the motion interval change of the output link ($\Delta\psi$) and the regulating link length change (Δl), is linear (i.e. $\Delta\psi = m \cdot \Delta l$), then the change of stroke S (as a function of the regulating link length change) is also linear, which is significant for regulation, meaning that:

$$\Delta S = iRm \cdot \Delta l = \text{const} \cdot \Delta l \quad (7)$$

The work coefficient (k) is the ratio between the periods of motion and dwell. The period of motion is the period during which the stacker panels move into position above the puncher, while the period of dwell refers to the period of product ejection, during which the stacker does not move. The change of the work coefficient due to changing the regulating link length (Δl) should be as small as possible, with the adopted limits being $\Delta k = \pm 5\%$.

Kinematic analysis

This section examines the possibility of fine tuning of the motion interval of the output link – angle ψ , as this would allow very high positioning precision of the ejection panels. Figure 3 shows the motion transformation mechanism in its initial and final position.

According to the equation (1) shown in Part I, the motion interval of the output link is calculated as:

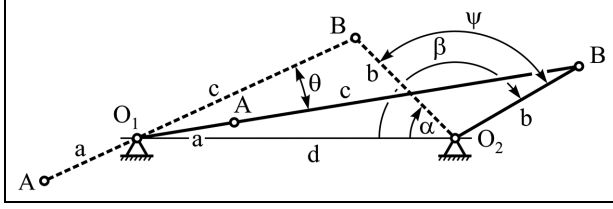


Figure 3. Mechanism for motion transformation – combination of four-bar linkage and one-way clutch.

$$\psi = \arccos\left(\frac{d^2 + b^2 - (c + a)^2}{2db}\right) - \arccos\left(\frac{d^2 + b^2 - (c - a)^2}{2db}\right) \quad (8)$$

According to equation (8), angle ψ can be changed by varying the length of all four of the links (a , b , c and d). Therefore, the length of any link can be the regulating parameter. However, it should be noted that every mechanism has one immobile – fixed link, presented as the distance between the two fixed points. From a design standpoint, this is the link whose length it is the easiest to make variable. Also, it is the only link whose length could be changed while the stacker is active. On the other hand, changing the distance between the two fixed points is not always the most rational solution. In this specific case, if the distance between the fixed points is variable, an additional variator is necessary to compensate for the change in distance between shafts, which largely complicates the solution and makes it more expensive. A more rational choice is to consider one of the moving links for the regulation link. An analysis of each moving link as a potential regulating link will be done.

Let the length of the output link b change by Δb . This will change the angles, with α and β becoming α_1 and β_1 . Therefore:

$$\cos(\alpha_1) = \frac{(b + \Delta b)^2 + d^2 - (c - a)^2}{2d(b + \Delta b)} \quad (9)$$

$$\cos(\beta_1) = \frac{(b + \Delta b)^2 + d^2 - (c + a)^2}{2d(b + \Delta b)} \quad (10)$$

Also, angle ψ will change to ψ_1 , which now equals:

$$\psi_1 = \arccos\left(\frac{(b + \Delta b)^2 + d^2 - (c + a)^2}{2d(b + \Delta b)}\right) - \arccos\left(\frac{(b + \Delta b)^2 + d^2 - (c - a)^2}{2d(b + \Delta b)}\right) \quad (11)$$

Therefore, the change of the motion interval of the output link is:

$$\Delta\psi_b = \psi_1 - \psi \quad (12)$$

Inserting equations (9)–(11) into equation (12) results in the following:

$$\begin{aligned} \Delta\psi_b = & \arccos\left(\frac{(b + \Delta b)^2 + d^2 - (c + a)^2}{2d(b + \Delta b)}\right) \\ & - \arccos\left(\frac{(b + \Delta b)^2 + d^2 - (c - a)^2}{2d(b + \Delta b)}\right) \\ & - \left(\arccos\left(\frac{d^2 + b^2 - (c + a)^2}{2db}\right) \right. \\ & \left. - \arccos\left(\frac{d^2 + b^2 - (c - a)^2}{2db}\right) \right) \end{aligned} \quad (13)$$

Similarly, equations that define the change of the motion interval due to the change in length of links c or a can be expressed as such:

$$\begin{aligned} \Delta\psi_c = & \arccos\left(\frac{d^2 + b^2 - (c + \Delta c + a)^2}{2db}\right) \\ & - \arccos\left(\frac{d^2 + b^2 - (c - \Delta c - a)^2}{2db}\right) \\ & - \left(\arccos\left(\frac{d^2 + b^2 - (c + a)^2}{2db}\right) \right. \\ & \left. - \arccos\left(\frac{d^2 + b^2 - (c - a)^2}{2db}\right) \right) \end{aligned} \quad (14)$$

$$\begin{aligned} \Delta\psi_a = & \arccos\left(\frac{d^2 + b^2 - (c + a + \Delta a)^2}{2db}\right) \\ & - \arccos\left(\frac{d^2 + b^2 - (c - a - \Delta a)^2}{2db}\right) \\ & - \left(\arccos\left(\frac{d^2 + b^2 - (c + a)^2}{2db}\right) \right. \\ & \left. - \arccos\left(\frac{d^2 + b^2 - (c - a)^2}{2db}\right) \right) \end{aligned} \quad (15)$$

Equations (13)–(15) can be used to form regulation characteristics which represent the change of the motion interval $\Delta\psi$ as a function of the regulation parameter Δb , Δc or Δa . Another point to consider is the change of the work coefficient – it must be within the prescribed limits. The work coefficient is defined as:

$$k = \frac{180^\circ + \theta}{180^\circ - \theta} \quad (16)$$

where:

$$\theta = \arcsin\left(\frac{b \cos \beta}{c - a}\right) - \arcsin\left(\frac{b \cos \alpha}{a + c}\right) \quad (17)$$

The work coefficient after changing b becomes:

$$k_b = \frac{180^\circ + \theta_b}{180^\circ - \theta_b} \quad (18)$$

where:

$$\theta_b = \arcsin\left(\frac{(b + \Delta b) \cos \beta_b}{c - a}\right) - \arcsin\left(\frac{(b + \Delta b) \cos \alpha_b}{a + c}\right) \quad (19)$$

where:

$$\cos(\alpha_b) = \frac{d^2 + (b + \Delta b)^2 - (c - a)^2}{2d(b + \Delta b)} \quad (20)$$

$$\cos(\beta_b) = \frac{d^2 + (b + \Delta b)^2 - (c + a)^2}{2d(b + \Delta b)} \quad (21)$$

Similarly, the work coefficient, if the regulation parameter is Δc , becomes:

$$k_c = \frac{180^\circ + \theta_c}{180^\circ - \theta_c} \quad (22)$$

where:

$$\theta_c = \arcsin\left(\frac{b \cos \beta_c}{c + \Delta c - a}\right) - \arcsin\left(\frac{b \cos \alpha_c}{a + c + \Delta c}\right) \quad (23)$$

where:

$$\cos(\alpha_c) = \frac{d^2 + b^2 - (c + \Delta c - a)^2}{2db} \quad (24)$$

$$\cos(\beta_c) = \frac{d^2 + b^2 - (c + \Delta c + a)^2}{2db} \quad (25)$$

And finally, if the regulation parameter is Δa :

$$k_a = \frac{180^\circ + \theta_a}{180^\circ - \theta_a} \quad (26)$$

where:

$$\theta_a = \arcsin\left(\frac{b \cos \beta_a}{c - a - \Delta a}\right) - \arcsin\left(\frac{b \cos \alpha_a}{a + \Delta a + c}\right) \quad (27)$$

where:

$$\cos(\alpha_a) = \frac{d^2 + b^2 - (c - a - \Delta a)^2}{2db} \quad (28)$$

$$\cos(\beta_a) = \frac{d^2 + b^2 - (c + a + \Delta a)^2}{2db} \quad (29)$$

Analysis of regulation parameters

The dimensions of the stacker mechanism will be determined by the optimization. In order to reduce the time and increase the efficiency of the optimization process, an approach similar to hybrid optimization methods will be applied,^{25,35,36} i.e. combining several procedures in order to obtain additional information on optimization parameters, constraints, etc. In accordance with that, before the optimization, an analysis examining the influence of the regulation parameter variation – the lengths of links a , b or c , on the change of the output link b rotation angle ψ , will be done.

An analysis of the regulation parameters was conducted for three configurations (C-1, C-2 and C3 – see Part I, Figure 6) and four motion intervals of the output link ($\psi_{sr} = 15^\circ, 30^\circ, 45^\circ$ and 60°). Table 2 shows the dimensions of the links for each configuration and value of angle ψ_{sr} . According to Part I, configuration C-3 combined with motion intervals of 45° and 60° yields a transmission angle γ below the prescribed lower limit, so these solutions are disregarded.

In order to compare the results, variable normalization will be performed. Instead of $\psi = \psi(l)$, the following will be considered:

$$\frac{\Delta \psi}{\psi_{sr}} = \frac{\Delta \psi}{\psi_{sr}} \left(\frac{\Delta l}{l_{sr}} \right) \quad (30)$$

where $\Delta \psi = \Delta \psi(\Delta l)$ and $\Delta l = l - l_{sr}$, where l is the length of links a , b , c .

It was previously pointed out that, for the regulation of parameters, it is very important that $\Delta \psi = \Delta \psi(\Delta l)$ be linear, i.e. $\Delta \psi = \Delta \psi(\Delta l) = m \cdot \Delta l$. This implies that through the entire regulation interval, for the same change of the link length, the same change of the angle ψ range is obtained. Therefore, to change the range of

Table 2. Design parameters of four-bar linkage mechanism.

ψ_{sr} [°]	Configuration	Link length		
		a_{sr} [m]	b_{sr} [m]	c_{sr} [m]
15	C-1	0.0547	0.4613	1.0999
	C-2	0.0597	0.4633	0.9619
	C-3	0.0518	0.4712	1.1714
30	C-1	0.0997	0.4154	1.0782
	C-2	0.1168	0.4537	0.9439
	C-3	0.0705	0.3182	1.1239
45	C-1	0.1394	0.3872	1.0632
	C-2	0.1814	0.4742	0.9132
60	C-1	0.1532	0.3180	1.0381
	C-2	0.2943	0.5886	0.8633

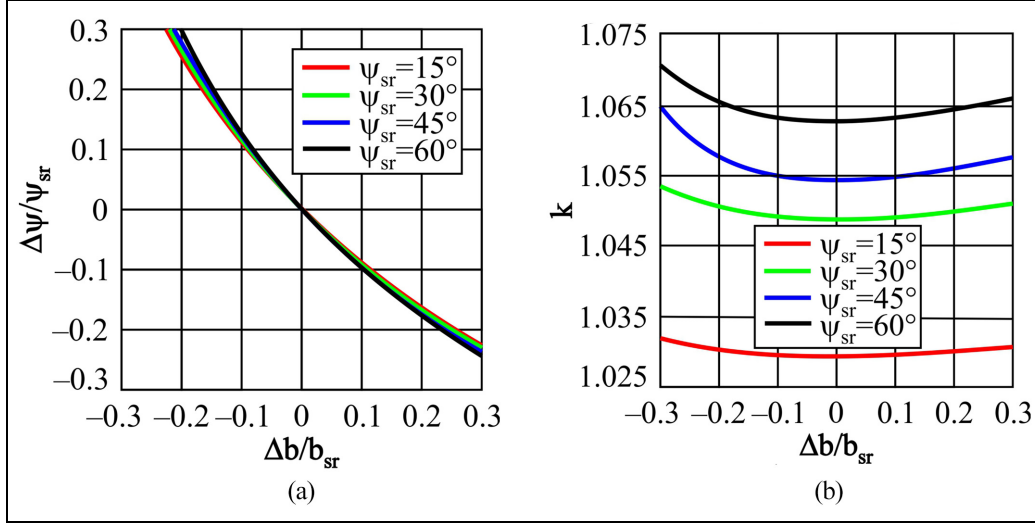


Figure 4. Configuration C-1: (a) change of the motion interval ψ and (b) work coefficient k , both functions of the change of regulation parameter b .

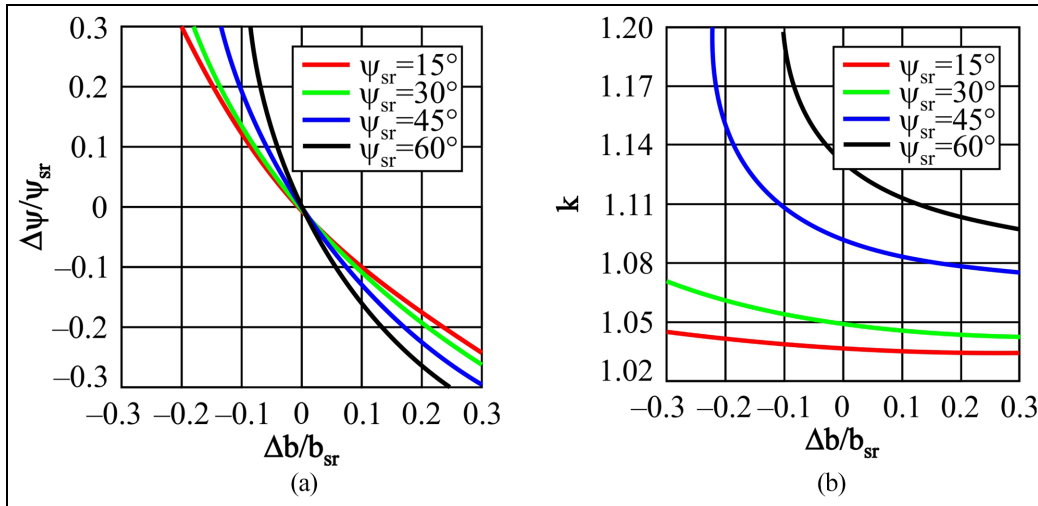


Figure 5. Configuration C-2: (a) change of the motion interval ψ and (b) work coefficient k , both functions of the change of regulation parameter b .

the angle ψ of 1° , the length of the link l should change by $1/m$ mm. On the example of a threaded spindle with a 1 mm pitch, if $m = 0.2$, the length of the link l should be changed by 5 mm, which is achieved with five full revolutions of the spindle, where the nut is fixed and immobile.

Variation of parameter b . The length of link b will vary from $b_{sr} - 0.3b_{sr}$ to $b_{sr} + 0.3b_{sr}$. According to equations (13) and (18), for each new value of b , new values of angle ψ and work coefficient k will be calculated. All three configurations will be analysed (C-1, C-2 and C-3). Figures 4(a), 5(a) and 6(a) show the dependency of

the motion interval ψ ($\Delta\psi/\psi_{sr}$) on the relative change in length of link b ($\Delta b/b_{sr}$), where:

$$\Delta b = b - b_{sr} \quad (31)$$

$$\Delta\psi = \psi - \psi_{sr} \quad (32)$$

Figures 4(b), 5(b) and 6(b) show the dependency of the work coefficient k on the relative change in length of link b ($\Delta b/b_{sr}$).

According to Figures 4 to 6, the required change of the motion interval $\Delta\psi = \pm 0.30\psi_{sr}$ can be achieved with configurations C-1 and C-2, and all four median values of the motion interval ($\psi_{sr} = 15^\circ, 30^\circ, 45^\circ$ and 60°), and with configuration C-3 and median values

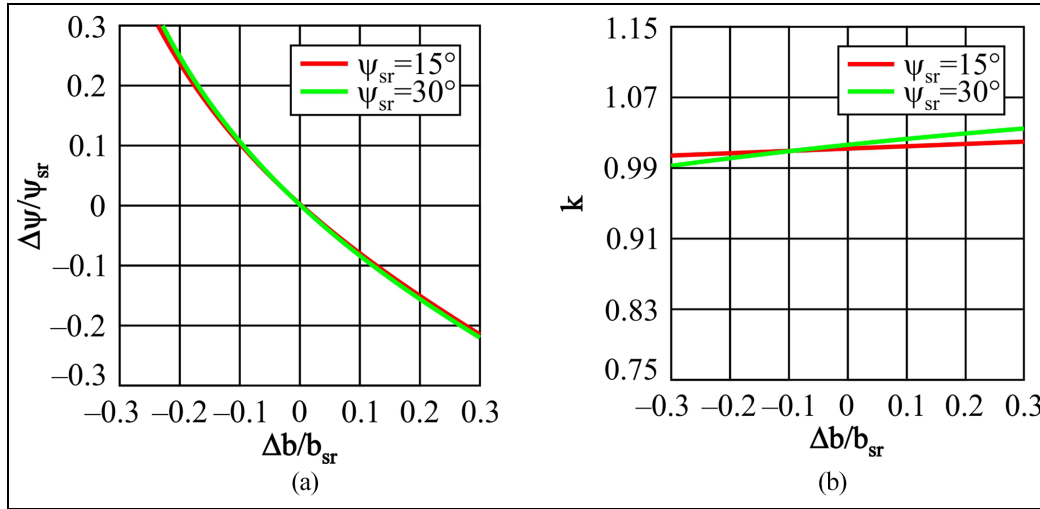


Figure 6. Configuration C-3: (a) change of the motion interval ψ and (b) work coefficient k , both functions of the change of regulation parameter b .

$\psi_{sr} = 15^\circ$ and 30° . Regardless, the obtained functions are nonlinear, which is unfavourable in the context of regulation. The $+0.30\psi_{sr}$ variation is achieved by decreasing the length of the output link b by approximately 20% for configurations C-1 and C-3, while for configuration C-2 the length is to be shortened less, by about 10–20%, depending on the median value of the motion interval ψ_{sr} . On the other hand, the $-0.30\psi_{sr}$ variation is achieved by lengthening the output link b by approximately 25–40% for configuration C-2, depending on the value of ψ_{sr} , while configurations C-1 and C-3 require the output link to be lengthened by over 40%. Furthermore, increasing the median value of the motion interval of the output link b increases the work coefficient. For configuration C-1, the work coefficient changes very little (compared to its value for $\psi = \psi_{sr}$), with the change being 0.5%, 1%, 2% and 3% for $\psi_{sr} = 15^\circ, 30^\circ, 45^\circ$ and 60° , respectively. Moving on, for configuration C-2 the changes are somewhat larger and equal approximately $0 \div 0.5\%$, $-0.5 \div 1\%$, $-1.5 \div 2.5\%$ and $-2.5 \div 4.5\%$ for $\psi_{sr} = 15^\circ, 30^\circ, 45^\circ$ and 60° , respectively. Finally, for configuration C-3, the work coefficient changes the most, while still being within the prescribed limits, the changes equalling $0.5 \div 1\%$ and $-3.5 \div 4.5\%$ for $\psi_{sr} = 15^\circ$ and 30° , respectively.

Variation of parameter c . The length of link c will vary from $c_{sr} - 0.3c_{sr}$ to $c_{sr} + 0.3c_{sr}$. According to equations (14) and (22), for each new value of c , new values of angle ψ and work coefficient k will be calculated. All three configurations will be analysed (C-1, C-2 and C-3). Figures 7(a), 8(a) and 9(a) show the dependency of the motion interval ψ ($\Delta\psi/\psi_{sr}$) on the relative change in length of link c ($\Delta c/c_{sr}$), where:

$$\Delta c = c - c_{sr} \quad (33)$$

$$\Delta\psi = \psi - \psi_{sr} \quad (34)$$

Figures 7(b), 8(b) and 9(b) show the dependency of the work coefficient k on the relative change in length of link c ($\Delta c/c_{sr}$).

According to Figures 7 to 9, for all three configurations (C-1, C-2 and C-3) and all four median values of the motion interval of the output link ($\psi_{sr} = 15^\circ, 30^\circ, 45^\circ$ and 60°), changing the length of the connecting link c yields strictly unfavourable results. Aside from the function $\Delta\psi/\psi_{sr}(\Delta c/c_{sr})$ being nonlinear, it is impossible to achieve the $-0.30\psi_{sr}$ variation with any of the configurations or motion intervals.

Variation of parameter a . The length of link a will vary from $a_{sr} - 0.3a_{sr}$ to $a_{sr} + 0.3a_{sr}$. According to equations (15) and (26), for each new value of a , new values of angle ψ and work coefficient k will be calculated. All three configurations will be analysed (C-1, C-2 and C-3). Figures 10(a), 11(a) and 12(a) show the dependency of the motion interval ψ ($\Delta\psi/\psi_{sr}$) on the relative change in length of link a ($\Delta a/a_{sr}$), where:

$$\Delta a = a - a_{sr} \quad (35)$$

$$\Delta\psi = \psi - \psi_{sr} \quad (36)$$

Figures 10(b), 11(b) and 12(b) show the dependency of the work coefficient k on the relative change in length of link a ($\Delta a/a_{sr}$).

According to Figures 10 to 12, the prescribed $\Delta\psi = \pm 0.30\psi_{sr}$ variation can be achieved for all four median values of the motion interval ψ_{sr} and for all three configurations. Changing the length of the input link a

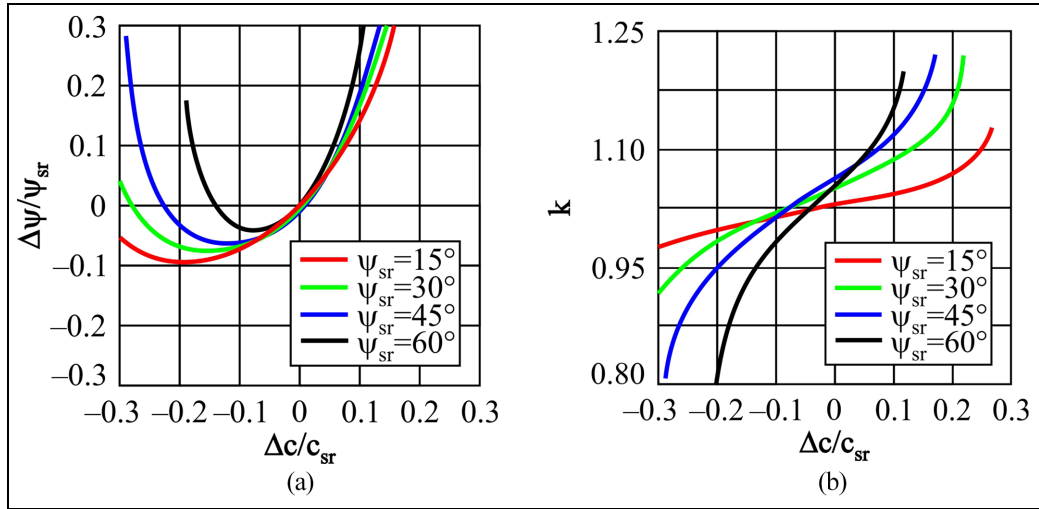


Figure 7. Configuration C-1: (a) change of the motion interval ψ and (b) work coefficient k , both functions of the change of regulation parameter c .

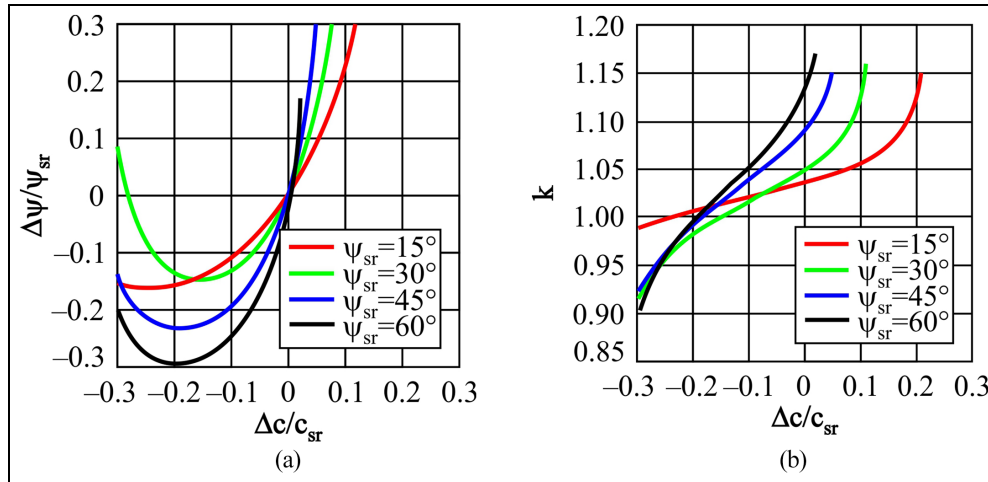


Figure 8. Configuration C-2: (a) change of the motion interval ψ and (b) work coefficient k , both functions of the change of regulation parameter c .

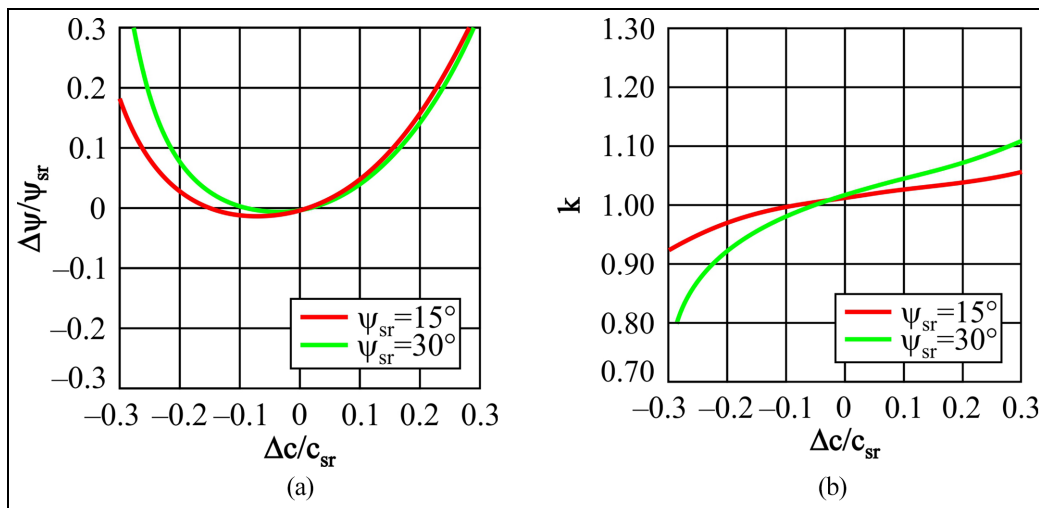


Figure 9. Configuration C-3: (a) change of the motion interval ψ and (b) work coefficient k , both functions of the change of regulation parameter c .

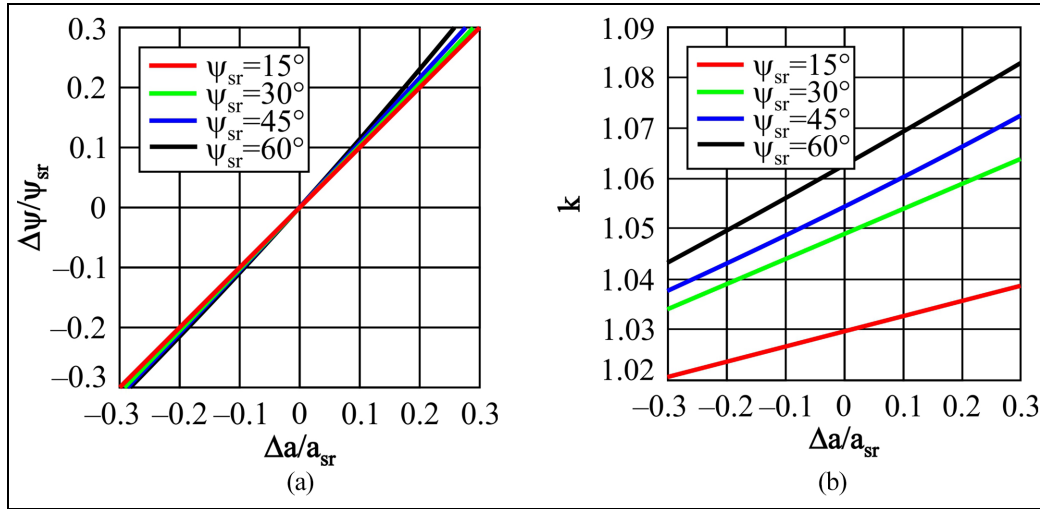


Figure 10. Configuration C-1: (a) change of the motion interval ψ and (b) work coefficient k , both functions of the change of regulation parameter a .

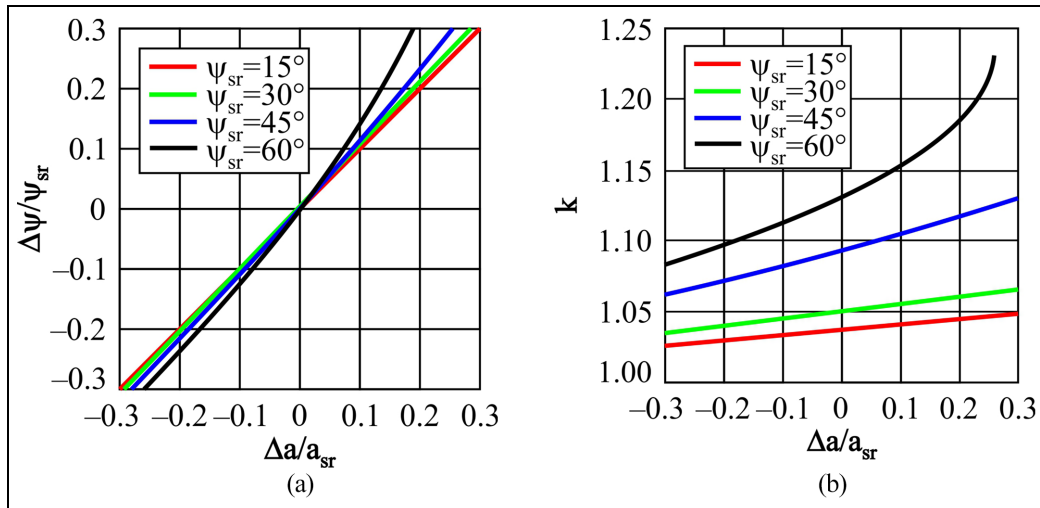


Figure 11. Configuration C-2: (a) change of the motion interval ψ and (b) work coefficient k , both functions of the change of regulation parameter a .

yields a symmetrical – nearly linear curve, for all the median values of the motion intervals and configurations C-1 and C-3, and for configuration C-2 and the median motion interval values of $\psi_{sr} = 15^\circ$, 30° and 45° . For larger median values of the motion interval ψ_{sr} , the variation $\Delta\psi = \pm 0.30\psi_{sr}$ can be achieved by changing the length of the input link a by less than 30%. Furthermore, the change of the work coefficient is miniscule, and in general grows in proportion with ψ_{sr} . The work coefficient changes (compared to its value for $\psi = \psi_{sr}$) by approximately $\pm 0.3\%$, $\pm 0.6\%$, $\pm 1\%$ and $\pm 1.5\%$ for configuration C-1. The values are similar for configurations C-2 and C-3 and $\psi_{sr} = 15^\circ$ and 30° , and slightly larger for these two configurations and $\psi_{sr} = 45^\circ$ and 60° .

Summarization. Based on the examination and analysis of the results obtained about the impact of changes in regulation parameters – links a , b and c , the following was concluded:

1. Changing the length of link c is not an option, because it is not possible to achieve the desired change of the rotation angle ψ interval of the output link b (see Figures 7(a), 8(a) and 9(a)). In addition, the resulting curves are similar to parabolas and deviate greatly from the desired one – the goal is linear change.
2. Changing the length of link b is a possible option for the given mechanism, but it is not appropriate, because changing the motion

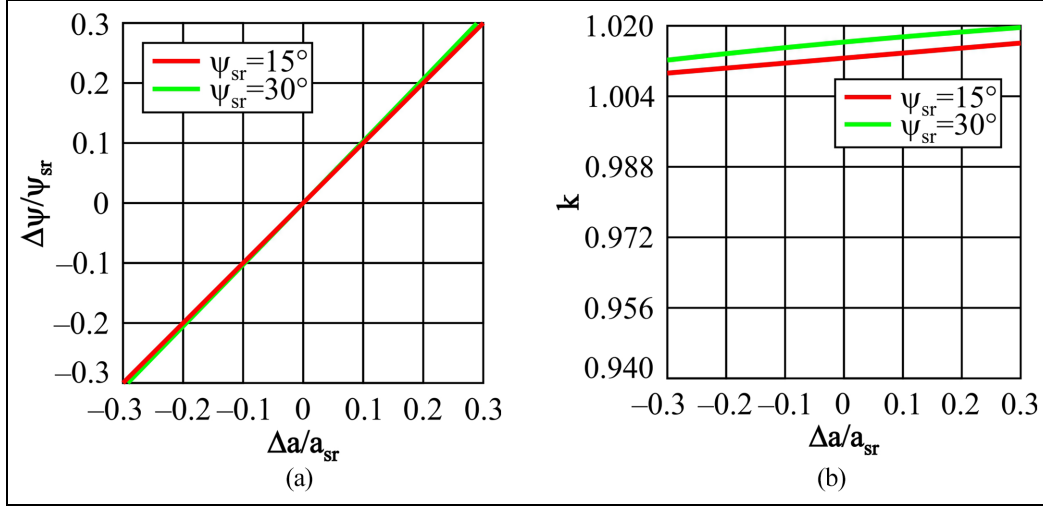


Figure 12. Configuration C-3: (a) change of the motion interval ψ and (b) work coefficient k , both functions of the change of regulation parameter a .

interval of angle ψ by $\pm 30\%$ is achieved by changing the length of link b by more than 40% , except for C-2 ($\psi_{sr} = 45^\circ$ and 60°). However, due to the very large change in the work coefficient k (see Figures 4(b), 5(b) and 6(b)), even the C-2 configuration is not appropriate.

3. The only viable option is to change the length of link a , where, theoretically, all configurations come into consideration. Changing the range of rotation angle ψ of the output link b by $\pm 30^\circ$ is achieved by changing the length of link a by close to $\pm 30\%$. The dependence is close to linear, while the work coefficient k changes within the prescribed limits (see Figures 10(b), 11(b) and 12(b)). However, when $\psi_{sr} = 60^\circ$, the angle change would be $\Delta\psi = \pm 20^\circ$, so the adjustable range of the angle is $\psi = 40^\circ \div 80^\circ$, and based on Part I analyses, for configurations with $\psi_{sr} = 60^\circ$, the transmission angle γ approaches the limit value. Also, with Figures 10(b) and 11(b), it is concluded that the work coefficient k changes significantly, nearly $\pm 5\%$, so it is not recommended to work with motion intervals of the output link close to 60° .

Optimization. In order to design a flexible stacker that will be able to accept and transport cup-like products of different dimensions (please see Table 1), it is necessary to provide adjustment of the conveyor stroke, which is achieved by changing one or more links of the stacker mechanism (see Figure 2). Based on section 4.2.4, it was concluded that the regulation of the work stroke of the conveyor will be done by changing the length of the input link a . It is necessary for each

mechanism, in the range of regulation $\pm 0.3\psi_{sr}$, to satisfy the condition of assembly of the mechanism, Grashof's conditions, as well as the corresponding values of the transmission angle γ and the work coefficient k . From a practical realization point of view, it is essential that the regulation curve on the entire interval of change of the conveyor work stroke (see Figure 1, distance S) be as close to linear as possible. Solving this problem requires compromises to be made for numerous parameters, which is why it is necessary to perform the optimization.

The optimization problem represents minimization of the objective function $F(x)$, $x \in D$ for the set constraints, where $x = (x_1, x_2, \dots, x_m)$ is the vector of variables, $D = \{x \in R_n \mid g(x) \leq 0 \wedge h(x) = 0\}$ is the set of solutions that fulfils the defined constraints, while $g(x) \leq 0$ and $h(x) = 0$ are the vectors of constraints.

For the purpose of efficient regulation and practical realization of stackers, the most suitable regulation curve is:

$$\frac{\Delta\psi}{\psi_{sr}} = m \frac{\Delta a}{a_{sr}} \quad (37)$$

Based on equation (30), the objective function is formed:

$$F = \sum_{i=1}^n \left(\frac{\Delta\psi_i}{\psi_{sr}} - m \frac{\Delta a_i}{a_{sr}} \right)^2 \quad (38)$$

where $\Delta a_i/a_{sr}$ changes in the interval $[-0.3, 0.3]$, while n is the number of intermediate points.

The parameters to be optimized are the lengths of the links b and c , where $0.3 < b < 0.6$ and $0.8 < c < 1.2$, as well as a_{sr} – the basic length of the link a , where $0.05 < a_{sr} < 0.3$. In order to solve the problem,

it is allowed to change the length of the ground link d in the range of $0.9 < d < 1.1$. According to production requirements the minimum value of link a is prescribed. The maximum values for links a and b are due to the allowed vertical dimension of the mechanism, while the values for link c are due to the allowed horizontal dimension of the mechanism. Also, it is allowed to change the angle ψ_{sr} within the limits of $40^\circ \leq \psi_{sr} \leq 50^\circ$, as well as the coefficient m where the limits of $0.9 \leq m \leq 1.1$ are allowed. Based on all this, the optimization parameter vector is:

$$x = [x_1 \ x_2 \ x_3 \ x_4 \ x_5 \ x_6] = [a_{sr} \ b \ c \ d \ \psi_{sr} \ m] \quad (39)$$

Each mechanism obtained for $\Delta a_i/a_{sr}$ must be possible to assemble and meet the Grashof's condition, where the work coefficient k must be in the range $1 < k < 1.5$, and the transmission angle γ , where $\gamma_{min} > 45^\circ$ and $\gamma_{max} < 135^\circ$. It is sufficient to check the extreme cases of the mechanisms, i.e. for $i = 1$ (the length of link a is the smallest) and $i = n$ (the length of link a is the largest).

The basic length of link a_{sr} should correspond to the angle ψ_{sr} , which is why this condition is prescribed:

$$\psi_{sr} = \arccos\left(\frac{d^2 + b^2 - (c + a_{sr})^2}{2bd}\right) - \arccos\left(\frac{d^2 + b^2 - (c - a_{sr})^2}{2bd}\right) \quad (40)$$

In order to realize the change of the angle ψ_{sr} by $\pm 30\%$, the conditions at the ends of the interval are prescribed:

$$\left|\frac{\Delta\psi_1}{\psi_{sr}}\right| \geq 0.3 \quad \text{and} \quad \left|\frac{\Delta\psi_n}{\psi_{sr}}\right| \geq 0.3 \quad (41)$$

Bearing in mind everything mentioned so far in section 4.3, a vector of constraints can be formed – the equation type constraints are:

$$h_1(x) = \psi_{sr} - \arccos\left(\frac{d^2 + b^2 - (c + a_{sr})^2}{2bd}\right) + \arccos\left(\frac{d^2 + b^2 - (c - a_{sr})^2}{2bd}\right) \quad (42)$$

$$h_1(x) = 180^\circ - \alpha_{sr} - \beta_{sr} \quad (43)$$

$$h_2(x) = \psi_{sr} - \arccos\left(\frac{d^2 + b^2 - (c + a_{sr})^2}{2bd}\right) + \arccos\left(\frac{d^2 + b^2 - (c - a_{sr})^2}{2bd}\right) \quad (44)$$

For the basic configuration C-2 there is only one constraint (equation 42), while for the basic configuration C-1 two constraints must be set, defined by equations (43) and (44).

Inequality type constraints apply to both basic configurations – these are:

$$g_1(x) = k_1 - 1.5 \quad (45)$$

$$g_2(x) = k_n - 1.5 \quad (46)$$

$$g_3(x) = 1 - k_1 \quad (47)$$

$$g_4(x) = 1 - k_n \quad (48)$$

$$g_5(x) = \gamma_{max\ 1} - 135^\circ \quad (49)$$

$$g_6(x) = \gamma_{max\ n} - 135^\circ \quad (50)$$

$$g_7(x) = 45^\circ - \gamma_{min\ 1} \quad (51)$$

$$g_8(x) = 45^\circ - \gamma_{min\ n} \quad (52)$$

$$g_9(x) = l_{min\ 1} + l_{max\ 1} - l_{s1\ 1} - l_{s2\ 1} \quad (53)$$

$$g_{10}(x) = l_{min\ n} + l_{max\ n} - l_{s1\ n} - l_{s2\ n} \quad (54)$$

$$g_{11}(x) = a_1 - b \quad (55)$$

$$g_{12}(x) = a_n - b \quad (56)$$

$$g_{13}(x) = a_1 - c \quad (57)$$

$$g_{14}(x) = a_n - c \quad (58)$$

$$g_{15}(x) = a_1 - d \quad (59)$$

$$g_{16}(x) = a_n - d \quad (60)$$

$$g_{17}(x) = a_{sr} - 0.3 \quad (61)$$

$$g_{18}(x) = 0.05 - a_{sr} \quad (62)$$

$$g_{19}(x) = b - 0.6 \quad (63)$$

$$g_{20}(x) = 0.3 - b \quad (64)$$

$$g_{21}(x) = c - 1.2 \quad (65)$$

$$g_{22}(x) = 0.8 - c \quad (66)$$

$$g_{23}(x) = 0.3 - \left|\frac{\Delta\psi_1}{\psi_{sr}}\right| \quad (67)$$

$$g_{24}(x) = 0.3 - \left|\frac{\Delta\psi_n}{\psi_{sr}}\right| \quad (68)$$

According to the presented equations, by applying the genetic algorithm method, the optimization was performed and the lengths of links a , b , c and d were obtained, as well as the value of parameter m , the function describing the change of angle ψ in relation to the change of length a , i.e. $\frac{\Delta\psi}{\psi_{sr}} \left(\frac{\Delta a}{a_{sr}}\right) = m \frac{\Delta a}{a_{sr}}$.

Table 3. Configuration C-2.

a_{sr} [m]	b [m]	c [m]	d [m]	ψ_{sr} [°]	m
0.1959	0.6000	0.8857	0.9000	40	1.0315

Table 4. Configuration C-1.

a_{sr} [m]	b [m]	c [m]	d [m]	ψ_{sr} [°]	m
0.0995	0.3000	1.1358	1.1000	40	1.0446

Results and discussion

Table 3 shows the optimization results for the C-2 configuration. The value of the objective function is $F = 2.53 \cdot 10^{-4}$. Even though the value of the objective function is relatively small, comparing the values of the real function $\frac{\Delta\psi}{\psi_{sr}} \left(\frac{\Delta a}{a_{sr}} \right)$ and the function obtained by the optimization $\frac{\Delta\psi}{\psi_{sr}} \left(\frac{\Delta a}{a_{sr}} \right) = m \frac{\Delta a}{a_{sr}}$, shows a difference of $\pm 1.5\%$. It should be noted that these differences are the highest near the ends of the regulation interval.

Table 4 shows the optimization results for the C-1 configuration. The value of the objective function is $F = 5.21 \cdot 10^{-4}$. There is also a difference between the values of the real objective function and the function obtained by the optimization – the difference is a bit larger and equals $\pm 2.5\%$, with the differences being the most pronounced near the ends of the regulation interval.

To decrease the differences, the optimization procedure was performed again with a slightly different objective function. The regulation characteristic is:

$$\frac{\Delta\psi}{\psi_{sr}} = m \frac{\Delta a}{a_{sr}} + n \quad (69)$$

Which makes the objective function:

$$F = \sum_{i=1}^n \left(\frac{\Delta\psi_i}{\psi_{sr}} - m \frac{\Delta a_i}{a_{sr}} - n \right)^2 \quad (70)$$

where n represents the newly included optimization parameter.

Table 5 shows the optimization results for the C-2 configuration. The value of the objective function is $F = 1.13 \cdot 10^{-4}$. The difference is now lower and equals $\pm 0.9\%$. The difference is the highest near the ends of the regulation interval, but it decreases rapidly, and for $\left| \frac{\Delta a}{a_{sr}} \right| = 0.25$, the absolute value of the difference falls below 0.5%. Although the result is not appropriate, the change is linear and de facto it is obtained that, to

Table 5. Configuration C-2.

a_{sr} [m]	b [m]	c [m]	d [m]	ψ_{sr} [°]	m	n
0.1959	0.6000	0.8857	0.9000	40	1.031	0.001516

Table 6. Configuration C-1.

a_{sr} [m]	b [m]	c [m]	d [m]	ψ_{sr} [°]	m	n
0.0994	0.3000	1.1358	1.1000	40	1.045	0.002147

change the angle ψ by 1° , it is necessary to change the length of the link by 4.46 mm.

Table 6 shows the optimization results for the C-1 configuration. The value of the objective function is $F = 1.13 \cdot 10^{-4}$. The difference is decreased to $\pm 1.3\%$. The difference is the highest near the ends of the regulation interval, but it decreases rapidly, and for $\left| \frac{\Delta a}{a_{sr}} \right| = 0.25$, the absolute value of the difference falls below 0.5%. In order to change the angle ψ by 1° , it is necessary to change the length of the link by 2.18 mm.

After analysing the regulation characteristics (see Figure 10(a) and Figure 11(a)), it becomes obvious that the smaller angle ψ_{sr} is, the function $\frac{\Delta\psi}{\psi_{sr}} \left(\frac{\Delta a}{a_{sr}} \right)$ has a more favourable shape. And truly, conducting the optimization procedure for $\psi_{sr} = 15^\circ$, for configuration C-1, yields $\frac{\Delta\psi}{\psi_{sr}} \left(\frac{\Delta a}{a_{sr}} \right) = 1.006 \frac{\Delta a}{a_{sr}} + 0.0002$, where the difference near the ends of the regulation interval equalling $\pm 0.1\%$. Similar results are obtained for configuration C-2.

According to the previous results, configurations with smaller motion intervals ($\psi_{sr} = 15^\circ$) are favourable from a practical realization standpoint for a system with a continuously variable length of the input link a . However, in the case of direct transmission from the OWC to the driving sprocket ($i = 1$), for the motion intervals $\psi_{sr} = 15^\circ$, the radius of the driving sprocket 7 (see Figure 1) exceeds 200 mm, making it too large. A solution for this issue is an addition of a gear pair with a transmission ratio $i < 1$. Although this does complicate the design, it is not overly problematic as a wide range of standard gearboxes is commercially available. A bigger problem is the backlash within the gearbox which can negatively influence the high precision positioning of the panels and the repeatability of the conveyor cycle, which should be taken into consideration when selecting the gearbox. On the other hand, configurations with larger motion intervals perform with the function $\Delta\psi/\psi_{sr} = m \cdot \Delta a/a_{sr} + n$. Although the value of n is fairly small, it must be taken into consideration. This complicates the realization of the system supplying

the variable length of the input link a , making it necessary to compensate for the n value.

It is clear that determining the optimal dimensions of the mechanism links is a compromise between two opposing requirements: (i) the need for the regulation characteristic to be linear $\Delta\psi/\psi_{sr} = m \cdot \Delta a/a_{sr}$ and (ii) the need for the regulation range of angle ψ_{sr} be as wide as possible. The optimal synthesis offers a balance between these two requirements. By limiting the minimum value of ψ_{sr} , the characteristic stays linear but has the following shape $y = m \cdot x + n$, necessitating the existence of a way to compensate the difference, which complicates the practical realization. The solution can be improved by further complicating the mechanism, i.e. by making two link lengths adjustable. One link would have discrete length change, with each specific length corresponding to a specific stroke value of the conveyor, while the fine tuning would be done with continuous variation of another links length. This approach fulfils both of the previously stated requirements. The minimum and maximum lengths of the first link allow for a wide regulation range, while the continuous change of the second link allows for fine tuning. Since the continuous change has a very narrow range, the linearity of the characteristic is ensured in the form $y = m \cdot x$. Figure 13 shows the described mechanism.

It should be noted that in order for the designed stacker to be compatible with all of the products listed in Table 1, four type of panels, i.e. four different strokes must be used. When stacking portion cups with a volume of $0.5 \div 1$ oz, type 1 panels are used. When stacking portion cups and cold cups with volumes of $1.5 \div 3$ oz and $4 \div 8$ oz, respectively, the products are received with type 2 panels. For portion cups and cold cups with volumes of $3.25 \div 5.5$ oz and $10 \div 16$ oz, respectively, type 3 panels are used. Finally, for cold cups with a volume of $8 \div 16$ oz, type 4 panels are used. Since the input link a is the shortest, it was adopted that its length would change discretely. The symmetrical motion of the output link b , the defining characteristic of configuration C-1, yields favourable values of the transmission angle γ and the work coefficient k , while the angular velocity and acceleration have a fairly uniform change with reasonable value extremes. According to previous discussions, the adopted motion interval is $\psi_{sr} = 45^\circ$. The regulation range is satisfactory, and the radius of the driving sprocket is an acceptable 125 mm (see equation 6). According to Table 2, for the motion interval $\psi_{sr} = 45^\circ$, the lengths of the link are: $a_{sr} = 139.4$ mm, $c = 1063.2$ mm and $b = 387.2$ mm. Accordingly, for the work stroke values $S_1 = 56$ mm, $S_2 = 72$ mm, $S_3 = 88$ mm and $S_4 = 104$ mm, keeping in mind equation (13), the corresponding lengths of the input link are: $a_1 = 99$ mm, $a_2 = 125.2$ mm, $a_3 = 151.5$ mm and $a_4 = 181.2$ mm. During the practical realization, link a should be made in such a way to

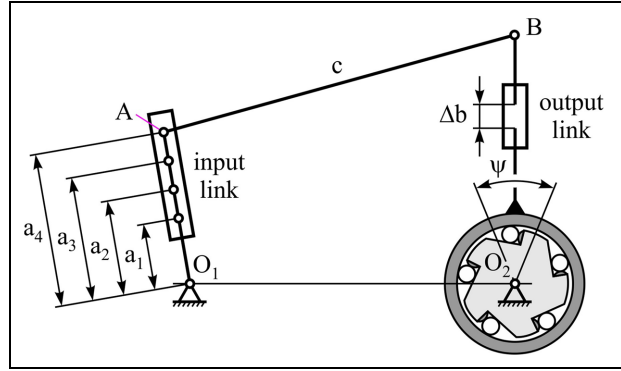


Figure 13. Motion transformation mechanism with two variable length links.

gain discrete length values. To simplify this process, the link lengths were standardized to: $a_1 = 99$ mm, $a_2 = 125$ mm, $a_3 = 152$ mm and $a_4 = 181$ mm. The difference between the standardized and non-standardized lengths is $\pm 1\%$, which will affect the accuracy of the work stroke. Another point is that the link will have to be manufactured within certain tolerances, which will further exacerbate the inaccuracy of the stroke. This makes the possibility of correction necessary, specifically the fine tuning of angle ψ (and the stroke). A mitigating circumstance here is that this fine tuning can be done with regulation within a very narrow range of $\pm 1.5\%$. Therefore, the fine tuning can be done by making the lengths of links b or c variable, and since both of these links are fairly large, they can be easily accessed, and allow for easy assembly and disassembly. Figure 7(a) shows that even small changes in the length of link c lead to a nonlinear change of angle ψ , so link b is selected as the regulation parameter. Finally, Figure 14 shows the change of the motion interval ψ ($\Delta\psi/\psi_{sr}$) as a function of the relative length change of link b ($\Delta b/b_{sr}$).

Changing angle ψ by $\pm 1.5\%$ is achieved by changing the length of b by $\pm 1.4\%$. Therefore, the change is linear, and for $\psi_{sr} = 45^\circ$, the following can be stated $\Delta\psi/\psi_{sr} = -1.055\Delta b/b_{sr} - 0.000005 = -1.055\Delta b/b_{sr}$, or rather, by changing b by 1 mm, the angle changes by 0.08° .

In light of all of this, the conclusion is that the solution shown in Figure 13 fulfils all of the stated requirements, as it enables both the intermittent motion of the conveyor and the possibility of achieving different work stroke values along with fine tuning. Since the four lengths of the input link a are discrete values, the practical realization is not complex. Although the length of link b needs to be varied continuously, due to its greater length the practical realization of this link is not problematic either. It should be noted that there is no need for an additional gearbox between the motion transformation mechanism 5 (see Figure 1) and the

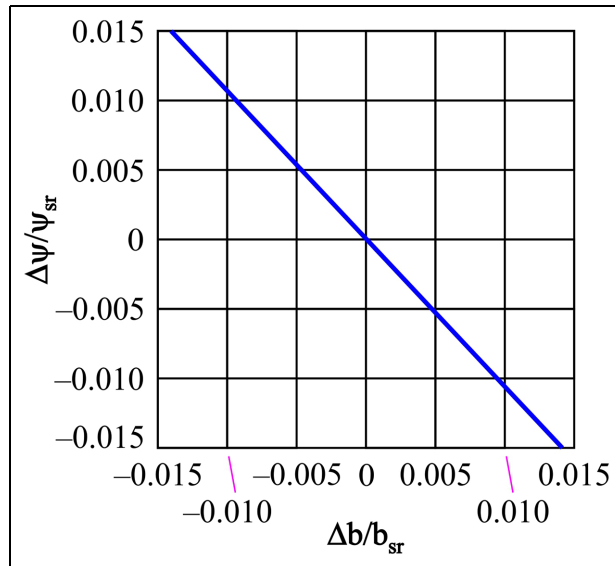


Figure 14. The change of the motion interval of the output link ψ as a function of the change in length of the output link b .

driving sprocket 7. Furthermore, the size of the driving sprocket is reasonable, so the adopted solution is satisfactory in the context of design and manufacturing complexity as well.

Conclusion

It should be noted that this paper is based on Part I, which shows the synthesis and further analysis of simple structure planar mechanisms with continuous rotation of the input link and oscillatory motion of the output link which, along with a one-way clutch, supply the conveyor with intermittent motion. It was concluded that a four-bar linkage with a one-way clutch was the most optimal solution.

Part II shows the structural design of a high-capacity adjustable mechanical stacker, which receives, transports and stacks cup-like products. The main objective was to enable the adjustment of the working parameters of the stacker, with the goal of changing and fine tuning the work stroke of the conveyor, which would make the stacker compatible with a wide array of different products. Based on an analysis of the most common product dimensions shown in Table 1, the necessary stroke values were obtained which would allow the stacker compatibility with all of the listed products, the limits being $S_{sr} \pm 0.3S_{sr}$. After analysing the results in Section 4, it was concluded that the solutions including variable lengths of the input and output links (a and b , respectively) were viable – change of a being preferable, while doing the solution with the variable length floating link was impossible.

The objective was to find the lengths a_{sr} , b , c and d , such that by continuously changing the length of the

input link $a = a_{sr} \pm \Delta a$ in a specific interval, the regulation characteristic had the following form $\Delta\psi/\psi_{sr} = m \cdot \Delta a/a_{sr}$. When the interval $\Delta\psi$ is wider (over 15°), there is a deviation near the ends of the interval, which is unfavourable both from a regulation and a practical realization point of view. Furthermore, it was shown that the regulation characteristic is described much better with the following equation $\Delta\psi/\psi_{sr} = m \cdot \Delta a/a_{sr} + n$. There are still deviations at the ends of the interval, but they are much smaller. Although coefficient n has a very low value, it still has to be taken into consideration for the practical realization, which is problematic, so it needs to be compensated for. Therefore, continuously changing the length of link a does not yield a precise and simple practical realization for the regulation of angle ψ – work stroke S , in a wider range. The solution can be improved by changing the length of two mechanism links. Link a has discrete values – a wide regulation range is ensured by the minimum and maximum length of link a . Link b can be changed continuously to provide fine tuning, to compensate for manufacturing and assembly errors. The continuous change of link length b is done within a very narrow range $\pm 1.5\%$, maintaining the linearity of the regulation characteristic in the form $y = m \cdot x$. The proposed solution is compatible with all of the products listed in Table 1. It should be noted that the necessary adjustments being made on the stacker for each product group are minimal and very fast to do. The production line does not halt when the stacker needs to be adjusted, since it takes less time to adjust the stacker than to change the mould of the thermoforming machine.

After realizing and implementing the described stacker, the research efforts will be directed to the examination of the regulation characteristics of the mechanism, the accuracy of panel positioning, as well as the structural stiffness and vibration sensitivity of the design. The final goal, of course, is to enable the packaging of grouped products with a mechanically controlled system, uniting the forming, stacking and packaging of cup-like products.



Declaration of conflicting interests

The author(s) declared no potential conflicts of interest with respect to the research, authorship, and/or publication of this article.

Funding

The author(s) received no financial support for the research, authorship, and/or publication of this article.

ORCID iDs

Marko Penčić  <https://orcid.org/0000-0002-2244-5698>
Maja Čavić  <https://orcid.org/0000-0002-3663-8458>

References

1. Čavić M, Penčić M, Oros D, et al. High-capacity stacking apparatus for thermoforming machine – Part I: Synthesis of intermittent mechanisms as stacker driving units. *Adv Mech Eng* 2021; 13: 1–18.
2. Hittig J and Wölk F-M. *Stacking apparatus for a thermoforming machine*. Patent US6241457B1, USA, 2001.
3. Wieser G and Knoll P. *Stacking station for a thermoforming plant, method for producing cup-shaped products and thermoforming plant*. Patent US10703583B2, USA, 2020.
4. Trautwein H, Eichbauer V and Wonzy M. *Method for stacking containers comprising thermoplastic, and apparatus for executing the method*. Patent US6692212B2, USA, 2004.
5. Lederer GH. *Stacking device*. Patent US3827582A, USA, 1974.
6. Wölk F-M and Zabel H. *Stacking apparatus for deep-drawn articles of plastics of plastics material*. Patent US4802808A, USA, 1989.
7. Benker J and Llewellyn P. *Thermoforming apparatus and method*. Patent US8021142B2, USA, 2011.
8. Padovani P. *Process and plant for handling thermoformed objects for a single-station thermoforming machine with formand cut mould*. Patent US6830425B2, USA, 2004.
9. Padovani P. *Method for thermoforming and stackeng hollow objects*. Patent US5453237A, USA, 1995.
10. Shao Y, Zhang W and Ding X. Configuration synthesis of variable stiffness mechanisms based on guide-bar mechanisms with length-adjustable links. *Mech Mach Theory* 2021; 156: 104153–1–104153–15.
11. Dutta S and Naskar TK. Synthesis of adjustable offset slider-crank mechanism for simultaneous generation of function and path using variable-length links. In: *1st International and 16th National Conference on Machines and Mechanisms (iNaCoMM 2013)*, Roorkee, India, 18–20 December 2013, pp. 465–471.
12. Krishnaraju A and Abdul Zubar H. Design and SAM analysis of reconfigurable four-legged mechanism using single degree of freedom. *Int J Heavy Veh Syst* 2021; 28: 242–261.
13. Choi B, Lee Y, Kim Y-J, et al. Development of adjustable knee joint for walking assistance devices. In: *IEEE/RSJ International Conference on Intelligent Robots and Systems (IROS 2017)*, Vancouver, BC, Canada, 24–28 September 2017, pp. 1790–1797. New York: IEEE Press.
14. Simionescu PA and Talpasanu I. Synthesis and analysis of the steering system of an adjustable tread-width four-wheel tractor. *Mech Mach Theory* 2007; 42: 526–540.
15. Wilhelm SR and Van de Ven JD. Design and testing of an adjustable linkage for a variable displacement pump. *J Mech Robot* 2013; 5: 041008–1–041008–8.
16. Olinski M, Gronowicz A and Ceccarelli M. Development and characterisation of a controllable adjustable knee joint mechanism. *Mech Mach Theory* 2021; 155: 104101–1–104101–14.
17. Alamdari A, Sovizi J, Jun SK, et al. Kinetostatic optimization for an adjustable four-bar based articulated leg-wheel subsystem. In: *IEEE/RSJ International Conference on Intelligent Robots and Systems (IROS 2014)*, Chicago, IL, USA, 14–18 September 2014, pp. 2860–2866. New York: IEEE Press.
18. Liu Y, Wang D, Yang S, et al. Design and experimental study of a passive power-source-free stiffness-self-adjustable mechanism. *Front Mech Eng* 2021; 16: 32–45.
19. Lucieer P and Herder JL. Design of an adjustable compensation mechanism for use in a passive arm support. In: *ASME International Design Engineering Technical Conferences and Computers and Information in Engineering Conference (IDETC/CIE 2005)*, Long Beach, CA, USA, 24–28 September 2005, pp. 491–500. ASME Press.
20. Thongsookmark C, Beckermann A, Hüsing M, et al. Kinematic design of an adjustable foot motion generator for gait rehabilitation. In: Venture G, Solis J, Takeda Y, et al. (eds) *ROMANSY 23 – robot design, dynamics and control (ROMANSY 2020)*. Cham: Springer, 2021, pp.297–304.
21. Soong R-C. A design method for four-bar mechanisms with variable speeds and length-adjustable driving links. *J Adv Mech Des Syst Manuf* 2009; 3: 312–323.
22. Daivagna UM and Balli SS. Synthesis of five-bar slider mechanism with variable topology for finitely separated positions. *Adv Mech Eng* 2011; 3: 697316–1–697316–10.
23. Govindasamy G, B.v CW and Rai RS. Dimensional synthesis of adjustable mechanism to generate square path verified by reconstructed adjustable parameter curve method. *AIP Conf Proc* 2020; 2270: 040009–1–040009–7.
24. Wang SJ and Sodhi RS. Kinematic synthesis of adjustable moving pivot four-bar mechanisms for multi-phase motion generation. *Mech Mach Theory* 1996; 31: 459–474.
25. Ganesan G and Sekar M. Optimal synthesis and kinematic analysis of adjustable four-bar linkages to generate filleted rectangular paths. *Mech Based Des Struct Mach* 2017; 45: 363–379.
26. Ibrayev S, Jomartov A, Tuleshov A, et al. Synthesis of four-bar linkage with adjustable crank length for multi-path generation. *Int J Mech Eng Robot Res* 2020; 9: 489–495.
27. Zhou H and Castillo T. Synthesis of adjustable linkages for precise path generation using the optimal pivot adjustment. In: *ASME International Design Engineering Technical Conferences and Computers and Information in Engineering Conference (IDETC/CIE 2008)*, Brooklyn, New York, USA, 3–6 August 2008, pp. 567–574. ASME Press.
28. Chanekar PV and Ghosal A. Optimal synthesis of adjustable planar four-bar crank-rocker type mechanisms for approximate multi-path generation. *Mech Mach Theory* 2013; 69: 263–277.
29. Zhou H and Cheung EHM. Adjustable four-bar linkages for multi-phase motion generation. *Mech Mach Theory* 2004; 39: 261–279.
30. Chang C-F. Synthesis of adjustable four-bar mechanisms generating circular arcs with specified tangential velocities. *Mech Mach Theory* 2001; 36: 387–395.
31. Govindasamy G, Rai RS and Rao GB. Optimal dimensional synthesis of rhombus path generating adjustable four-bar mechanism. In: Akinlabi E, Ramkumar P and

- Selvaraj M (eds) *Trends in mechanical and biomedical design (ICMechD 2019)*. Singapore: Springer, 2021, pp.71–82.
32. Zhou H, Jamal M and Mohammed A. Optimal synthesis of adjustable linkages for precise continuous path generation using the optimal link length adjustment. In: *ASME International Mechanical Engineering Congress and Exposition (IMECE 2008)*, Boston, MA, 31 October–6 November 2008, pp. 833–840. ASME Press.
 33. Balcerowiak D and Hopmann C. Homogenisation of the wall thickness distribution of thermoformed cups by using different pre-stretch plugs and process parameter settings to improve material efficiency. In: Hopmann C and Dahlmann R (eds) *Advances in Polymer Processing 2020: Proceedings of the International Symposium on Plastics Technology*. Berlin, Heidelberg: Springer Vieweg, 2020, pp. 79–92.
 34. Oliman ZM. *Scanfill sheet as alternative material in the thermoforming industry in the Philippines: an exploratory study*. MSc thesis. Lund: Lund University, 2014.
 35. Govindasamy G, Rao GB and Rai RS. Optimal dimensional synthesis of double-semi-circle and double-semi-ellipse path generating adjustable four-bar mechanisms. In: Akinlabi E, Ramkumar P and Selvaraj M (eds) *Trends in mechanical and biomedical design (ICMechD 2019)*. Singapore: Springer, 2021, pp.97–107.
 36. Govindasamy G, Wilson C and Neeraj K. Kinematic analysis and dimensional synthesis of filleted-rhombus path generating adjustable four-bar mechanism. In: Akinlabi E, Ramkumar P and Selvaraj M (eds) *Trends in mechanical and biomedical design (ICMechD 2019)*. Singapore: Springer, 2021, pp.139–148.